Journal of Materials and Environmental Science
ISSN : 2028-2508
e-ISSN : 2737-890X
CODEN : JMESCN

J. Mater. Environ. Sci., 2022, Volume 13, Issue 04, Page 409-423

http://www.jmaterenvironsci.com

Theoretical study of alkyl nitroindazole and aryl acetonitrile derivatives to predict the reactivity and selectivity of their reaction by the DFT method

Bahija Rebbah[1], Zakaria Jalil[2], Abderrahim El haib[3], Mohamed Mbarki[2], Abdellah Hannioui[1], El Mostapha Rakib[1]

[1]*Laboratory of Molecular Chemistry, Materials and Catalysis, Faculty of Science and Technology, Sultan Moulay Slimane University, B.P. 523, Beni-Mellal, Morocco*

[2]*Engineering Laboratory in Chemistry and Physics of Matter, Faculty of Science and Technology, Sultan Moulay Slimane University, B.P. 523, Beni-Mellal, Morocco*

[3]*Laboratoire de Chimie des Substances Naturelles, Faculté des Sciences Semlalia, Université Cadi Ayyad, B.P. 2390, Marrakech, Morocco*

Received 10 April 2022,
Revised 29 April 2022,
Accepted 30 April 2022

Keywords
- ✓ Alkyl nitroindazole,
- ✓ Aryl acetonitrile,
- ✓ Reactivity,
- ✓ Selectivity,
- ✓ DFT,
- ✓ GIAO,
- ✓ ESP,
- ✓ IR, RMN.

m.mbarki@usms.ma
Phone: +212 708630400

Abstract

To investigate the reactivity of organic molecules that have been synthetized from alkyl nitro indazole and aryl acetonitrile derivatives, using the B3LYP (Lee-Yang-Parr three-parameter Becke) exchange-correlation hybrid functional at the 6-311G (d, p) level, the present work have calculated global quantum descriptors (global reactivity indices), local quantum descriptors (using the Fukui function), electrostatic potential (ESP) maps, IR spectra frequencies and 1H and 13C NMR (by GIAO method) chemical shifts. Our results show that the experimental regioselectivities are correctly reproduced by the Fukui function. Indeed, the local nucleophilicity indices predict that the (O19, O20) and (O17, O18) oxygens atoms of A1 and A2 reactants, respectively, are more reactive than others. The C10, C10, and C11 carbons, of the CH_2 alkyl in B1, B2, and B3 reactants, respectively, have higher electrophilicity indices. These oxygen and carbon atoms show that they are the most active sites. The IR frequencies of the organic functions and the NMR chemical shifts of the 1H proton and 13C carbon are in better agreement with the experimental data.

1. Introduction

Indazole compounds, as substituted heterocyclic compounds, are well known used in medicinal organic chemistry [1, 2] and in various medicines [3], as these heterocycles impart a unique physical and biological properties to organic compounds [4]. Indazole and its derivatives are widely used as intermediary to synthesize targeted organic compounds; including agrochemicals, dyes, photographic chemicals and corrosion inhibitors. They are sparingly soluble in water and present antibacterial, antifungal, antiprotozoal and anthelmintic properties [5, 6, 7]. The indazole core is present in many molecules having biological activities [8] such as: analgesic, antimycotic, antibiotic, antiulcer and antitumor [9, 10, 11]. Indazoles are also anti-inflammatory agents, blood pressure regulators and also useful ligands in coordination chemistry [12]. The indazole cyclic system exercises an important function in biology, chemistry and pharmaceutical and veterinary products. Thus, the synthesis of indazole cyclic containing compounds is an important field of scientific research [8].

In 2015, Assoman Kouakou and his team reported the synthesis and characterization of the following molecules: C1: 2-(7-Hydroxyimino-1-methyl-1,7-dihydro-indazol-4-ylidene)-2-(p-tolyl)-acetonitrile, C2: 2-(7-Hydroxyimino-1-methyl-1,7-dihydro-indazol-4-ylidene)-2-(4-methoxy-phenyl) -acetonitrile, C3: 2-(4-Chloro-phenyl)-2-(7-Hydroxyimino-1-methyl-1, 7-dihydro-indazol-4-ylidene)- acetonitrile, C4: 2-(1-Ethyl-7-Hydroxyimino-1,7-dihydro-indazol- 4-ylidene)-2-(4-methoxy-phenyl)- acetonitrile and C5: 2-(4-Chloro-phenyl)-2-(1-ethyl-7-hydroxyimino-1,7-dihydro-indazol-4-ylidene)- acetonitrile [13]. These molecules are synthesized from the following reagents: alkyl nitro indazole (A1: 1-Methyl-7-nitro-1H-indazole, A2: 1-Ethyl-7-nitro-1H-indazole) and aryl acetonitrile derivatives (B1: 4-methyl-phenyl-acetonitrile, B2: 4-methoxy-phenyl-acetonitrile and B3: 4-Chloro-phenyl-acetonitrile) in alkaline medium according to the following equation (Figure 1):

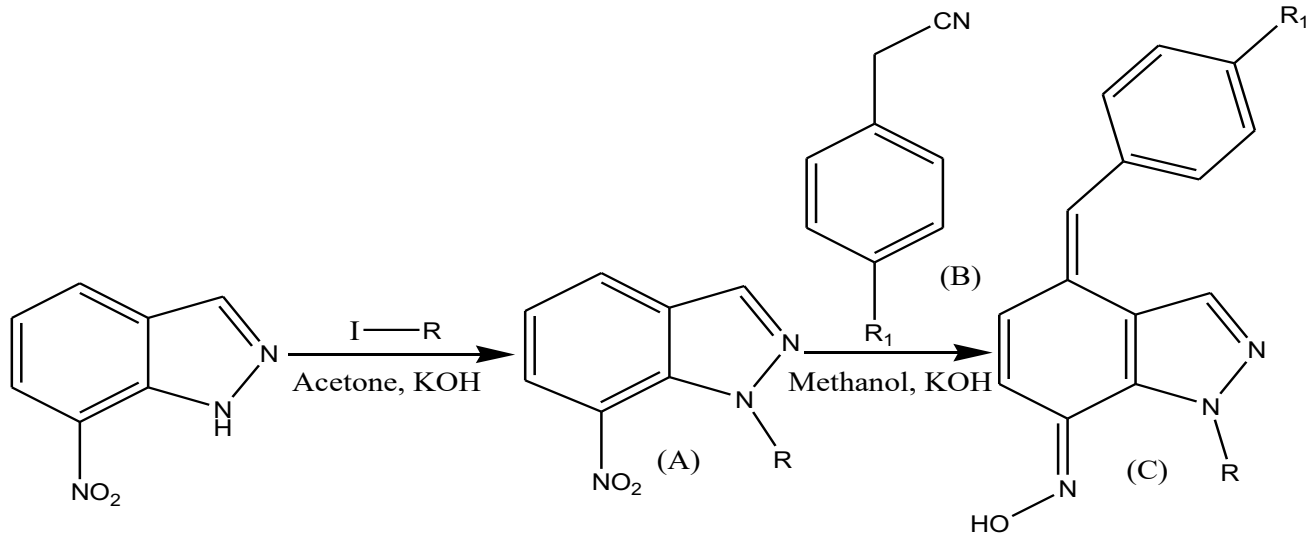

R	R1	C1 (A1+B1)	C2 (A1+B2)	C3 (A1+B3)	C4 (A2+B2)	C5 (A2+B3)
CH_3, CH_2-CH_3	CH_3, O-CH_3, Cl	CH_3/CH_3	CH_3/O-CH_3	CH_3/Cl	CH_2-CH_3/ O-CH_3	**CH_2-CH_3/Cl**

Figure 1. Nucleophilic substitution reaction between studied alkyl nitroindazole and aryl acetonitrile

The synthesized molecules bearing nitrile function have very important biological activities, such as: an interesting antiproliferative activity, relatively better inhibitory effects, the most potent cytotoxic activity against target cells by inducing cell apoptosis and stopping the cell cycle. They can be considered as promising medicine applied in anticancer medicine development [14]. They have a good antiproliferative/apoptotic activity that is pharmacologically interesting in humans [13, 15], inhibition of murine hepatic glucosidase [16] and showed inhibitory biological activity against *Aureus* [17]. Quantum chemistry, as a discipline integrating the principles of green chemistry, continues to gain the interest of both researchers and industrialists. Thanks to quantum chemistry, as a branch of theoretical chemistry, one can direct the experiment in organic chemistry and optimize the operating procedures of organic chemical synthesis. In fact, describing the electronic behavior of atoms and molecules and its effect on their ability to react is an application of quantum chemistry. The main objective of this work is to carry out a quantum and experimental study of the reactivity between molecules of the alkyl nitroindazole type on the one hand and molecules of the aryl acetonitrile type on the other hand. Such a study contributes to highlighting the more or less dialectical relationship that exists between theoretical chemistry and chemical experience. In order to be able to study these molecules, we have carried out the present work. Quantum chemical calculations shed light on molecular structures, orbital interactions, electronic and vibrational properties. More precisely, we have used the density functional

theory (DFT) that is a cost effective and reliable method [18, 19, 20]. This method provides a detailed information of the chemical descriptor of the molecule [21]. Since DFT was taught by the Hohenberg-Kohn theorem, it has become the most widely used method in chemistry and physics [22]. The DFT/B3LYP model presents good results in terms of electronic affinities binding energy and reasonably good performances before it concerns the vibrational frequencies and the geometrical structures of organic compounds [18, 19, 21, 23]. In the present work, we are interesting in the study of the nucleophilic/electrophilic properties of the A1, A2, B1, B2 and B3 reagents and the structural properties of the (C1, C2, C3, C4 and C5) synthetized molecules. In order to compare the reactivity of both the reactants and the synthetized molecules, we used the DFT method to calculate the relative reactivity (in terms of optimization of geometries, energy and density of HOMO and LUMO boundary molecular orbitals, chemical potential, electronegativity, chemical hardness, global softness, global electrophile index and global nucleophile index), the regioselectivity of the reactions (by the fukui function) and the molecular electrostatic potential.

2. Methodology

All calculations have been performed using the GAUSSIAN 09, program based on the B3LYP / 6-311G (d, p) level [24]. The geometry of all structures, the electrostatic potential, the IR frequencies of the organic functions and the NMR spectra have been optimized at this theoretical level. Thus, the calculations have been carried out also to determine both global and local quantum descriptors of the reagents and the spectroscopy of the studied molecules.

2.1 Global quantum descriptors

2.1.1 Chemical hardness η and softness S

The hardness of a product is a qualitative indication of its polarization or how its electron cloud is deformed in an electric field. Hardness has been presented in the literature [25, 26] to refer to the resistance to deformation by mechanical force. This explains the energy changes associated with the transition state to the ground state using different descriptors. Softness is the opposite of hardness. The overall hardness is given by the expression:

$$\eta = E_{LUMO} - E_{HOMO} \qquad \textbf{Eqn. I}$$

The chemical softness is given by the expression:

$$S = \frac{1}{2 * \eta} \qquad \textbf{Eqn. II}$$

2.1.2 Electronegativity χ

Electronegativity is the tendency of molecules to capture electrons [27]. In fact, Parr and Yang attempted to quantify this same descriptor [21]. This is represented by the average of the HOMO and LUMO energy values. This can be explained by the orbital energy terms at the boundaries.

$$\chi = -(E_{HOMO}+E_{LUMO})/2 \qquad \textbf{Eqn. III}$$

2.1.3 Chemical potential μ

The chemical potential (μ) represents the affinity of an electron to escape and is expressed as the first derivative of the total energy with respect to the number of electrons in a molecule [28]. According to the molecular orbital theory, μ is the inverse of the electronegativity value. It is given as follows:

$$\mu = \left(\frac{E_{HOMO} + E_{LUMO}}{2}\right) \qquad \textbf{Eqn. IV}$$

2.1.4 Electrophilicity index ω

The ability of a substance to accept electrons is quantified by the electrophilicity index (ω) [29]. Electron affinity is defined as the ability of a substance to have only one electron from the environment. This index measures the reduction in energy of a substance due to the flow of electrons between donor and acceptor.

The electrophilicity index and electron affinity (A) are measured by the following relations:

$$\omega = \frac{\mu^2}{2\eta} \quad \text{with} \quad A = -E_{LUMO} \qquad \textbf{Eqn. V}$$

2.1.5 Nucleophilic index N

The empirical (relative) nucleophilicity index, considered as a quantity, can be a measure of the electrophilic power of a system [29]. The empirical nucleophilicity index (Nu) is expressed, based on the HOMO energies found in the Kohn-Sham scheme, as:

$$N = E_{HOMO(Nu)} - E_{HOMO(TCE)} \qquad \textbf{Eqn. VI}$$

This nucleophilicity scale considers tetracyanoethylene (TCE) as the reference. This choice is expressed by managing a nucleophilicity scale with only positive values [30], since the value of E (HOMO (TCE)) is -9.3686 eV.

2.2 Local quantum descriptors

In order to differentiate the reactive behaviours of atoms within a molecule, we used the parameters of local reactivity. Among these parameters, we chose the Fukui function since it is the most commonly used. The local reactivity and regioselectivity of a reaction are explained by the numerical values of the Fukui function: The active site of nucleophilic attacks is the atom presenting the highest value of the local electrophilic index ω, while the electrophilic attack site is the atom that present the highest value of the local nucleophilic index N [31, 32]. In a non-polar reaction between two alternative reagents, the interaction will take place at the two most favourable active sites.

The Fukui Function, that measures the sensitivity of a system's chemical potential to an external perturbation at a particular site, is defined as [33]:

$$f(\vec{r}) = \left(\frac{\partial \rho(\vec{r})}{\partial N}\right)_{v\vec{r}} = \left(\frac{\partial \mu}{\partial v(\vec{r})}\right)_N \qquad \textbf{Eqn. VII}$$

Since the above derivatives are discontinuous, three different types of Fukui Function have been defined [33] :

$$f^{+}(\vec{r}) = \rho_{N+1}(\vec{r}) - \rho_N(\vec{r}), \text{ for nucleophilic attack} \qquad \textbf{Eqn. VIII}$$

$$f^{-}(\vec{r}) = \rho_N(\vec{r}) - \rho_{N-1}(\vec{r}), \text{ for electrophilic attack} \qquad \textbf{Eqn. IX}$$

$$f^{\circ}(\vec{r}) = (\rho_{N+1}(\vec{r}) - \rho_{N-1}(\vec{r}))/2, \text{ for radical attack} \qquad \textbf{Eqn. X}$$

3. Results and Discussion

3.1 Prediction of relative reactivity of reactants and polarity of nucleophilic substitution reactions

To determine the polar character in a reaction, one can use the difference of the global electrophilic indices of the reagents. Moreover, the present study has been carried out on the nucleophilic substitution reaction by the DFT method to establish the polar and non-polar character of the reactions [31]. The calculated values of the global reactivity indices for the reagents (namely: electronic chemical

potential, global hardness η, global electrophilicity ω, global nucleophilicity N and global maximum charge transfer ΔNmax) are presented in **Table1**.

Table 1. Global reactivity indices of the nucleophilic substitution reaction by the DFT/B3LYP method, for the alkyl nitroindazole and aryl acetonitrile reagents

Molecule	HOMO (eV)	LUMO (eV)	μ (eV)	η (eV)	ω (eV)	S (eV)	Egap (eV)	A (eV)	N(eV)	ΔNmax
A1	-6 .718944	-2 .82736	-4.773152	3.891584	2.927211	0.128482	3.891584	2.82736	2.649656	1.2265319
A2	-6 .615584	-2.757808	-4.686696	3.857776	2.846862	0.129608	3.857776	2,757808	2.753016	1.2148691
B1	-6.876976	-0.598672	-3.737824	6.278304	1.112667	0.079639	6.278304	0.598672	2.491624	0.5953556
B2	-6.41784	-0.710192	-3.564429	5.706820	1.113155	0.087614	5.707648	0.710192	2.95076	0.6245911
B3	-7.153882	-1.146208	-4.150045	6.007674	1.433406	0.083226	6.007674	1.146208	2.234718	0.6907906

In the case of the nucleophilic substitution reaction, the values of the electronic potential of the reactants B1, B2 and B3 of the aryl acetonitrile derivatives are: -3.737824, -3.564429 and -4.150045 eV, respectively. They are higher than the values of the -4.773152 and -4.686696 eV, electronic potential of the A1 and A2 alkyl nitroindazoles, respectively. These results indicate that electron transfer will take place from the aryl acetonitrile derivatives to the alkyl nitro indazoles. Moreover, the values of the global electrophilicity index of the aryl acetonitrile derivatives (1.112667 eV) are lower than those of the global electrophilicity index of the alkyl nitro indazole (2.927211 eV). It is noticed that the aryl acetonitrile derivatives (B1, B2 and B3) are considered as nucleophiles while the alkylnitroindazole (A1, A2) behave as electrophiles. Furthermore, the ΔNmax index, that represents the maximum charge ratio (ΔNmax = - μ/η) and that can be acquired by a system from its environment, has maximum values for alkyl nitroindazole (1.2265319) and minimum values for arylacetonitrile derivatives (0.5953556). So the electrophilic difference Δω and the difference between the HOMO energies of arylacetonitrile and LUMO derivatives of alkyl nitroindazole and their energy inverse are presented in **Table 2**.

Table 2. Difference between the two possible combinations HOMO/LUMO and Δω(eV)

Reactions	Reagents	X*(eV)	Y** (eV)	Δω (eV)
1	B1	4.049616	6.120272	-1.814544
2	B2	3.59048	6.008752	-1.814056
3	B3	1.326522	5.572736	-1.493805
4	B2	3.660032	5.905392	-1.733707
5	B3	4.396074	5.469376	-1.413456

***X=** $|E_{HOMO}^{B} - E_{LUMO}^{A1, A2}|$ **Eqn. XI**

****Y=** $|E_{HOMO}^{A1, A2} - E_{LUMO}^{B}|$ **Eqn. XII**

Table 2 shows that the **Y** energies are higher than the **X** energies. In the studied reactions, alkyl nitroindazole (A1 and A2) behaves as electrophile (electron acceptor) while aryl acetonitrile derivatives (B1, B2 and B3) behaves as nucleophile (electron donors). One can observe that the electrophilic difference (Δω) varies from -1.81 to -1.49 eV. In fact, all the studied reactions have a non-polar character thanks to their electrophilic difference values that are less than 1 (Δω<1) [32].

3.2 Prediction of the regioselectivity of the studied nucleophilic substitution reactions

The local electrophilic and nucleophilic abilities of alkyl nitro indazole and aryl acetonitrile are calculated thanks to the Fukui function using spin atomic density **(Table 3)**.

Table 3. Local electrophilic ability ω^+ and local nucleophilic ability ω^- of reagents A1, A2, B1, B2 and B3

Molecules	Atoms	N	N+1	N-1	f^+	f^-	ω^+	ω^-
A1	C1	-0,02654	0,008855	-0,04363	0,035394	0,017088	0,103606	0,045277
	C2	0,03884	0,066663	0,025905	0,027823	0,012935	0,081444	0,034273
	C3	0,032809	0,104516	0,018793	0,071707	0,014016	0,209902	0,037138
	C4	0,021966	0,13567	-0,0194	0,113704	0,041366	0,332836	0,109606
	C5	0,040699	0,161274	-0,01276	0,120575	0,053463	0,352948	0,141659
	C6	0,064454	0,228524	0,034927	0,16407	0,029527	0,480268	0,078236
	N10	-0,16534	-0,09686	-0,18584	0,068479	0,020497	0,200452	0,05431
	N11	0,002421	0,105342	-0,00276	0,102921	0,005179	0,301271	0,013723
	C12	0,160424	0,26889	0,127702	0,108466	0,032722	0,317503	0,086702
	C16	0,02736	0,102907	-0,02546	0,075547	0,052815	0,221142	0,139942
	N18	0,184176	0,196295	0,003385	0,012119	0,180791	0,035475	0,479034
	O19	-0,19057	-0,14108	-0,46031	0,049487	0,269741	0,144859	0,714721
	O20	-0,19076	-0,14104	-0,46063	0,049713	0,26987	0,14552	0,715063
A2	C1	-0,02721	0,01159	-0,05941	0,038803	0,032198	0,1104668	0,088642
	C2	0,046321	0,074074	0,020099	0,027753	0,026222	0,079009	0,07219
	C3	0,025434	0,098839	-0,01484	0,073405	0,040278	0,2089739	0,110886
	C4	0,017037	0,140631	-0,04941	0,123594	0,066444	0,3518551	0,182921
	C5	0,054031	0,162821	-0,06712	0,10879	0,121153	0,3097101	0,333536
	C6	0,072585	0,232335	0,018518	0,15975	0,054067	0,4547862	0,148847
	N10	-0,15265	-0,09299	-0,19642	0,059651	0,04377	0,1698182	0,1205
	N11	0,008275	0,109784	-0,00579	0,101509	0,014061	0,2889821	0,03871
	C12	0,104132	0,183304	0,083848	0,079172	0,020284	0,2253918	0,055842
	C15	0,033285	0,101675	-0,07539	0,06839	0,10867	0,1946969	0,29917
	N17	0,226666	0,245001	0,106555	0,018335	0,120111	0,0521972	0,330668
	O18	-0,2122	-0,17101	-0,37163	0,041184	0,159436	0,1172452	0,43893
	O19	-0,22353	-0,17315	-0,39324	0,050381	0,16971	0,1434278	0,467214
	C20	0,027839	0,077115	0,004238	0,049276	0,023601	0,140282	0,064974
B1	C1	0,003352	0,126752	-0,18321	0,1234	0,186561	0,137303	0,46484
	C2	0,00111	0,132271	-0,0508	0,131161	0,051908	0,145939	0,129335
	C3	0,003439	0,128147	-0,16992	0,124708	0,173355	0,138758	0,431935
	C4	0,006653	0,121089	-0,18029	0,114436	0,186945	0,127329	0,465797
	C5	-0,00856	0,119676	-0,05887	0,128237	0,050312	0,142685	0,125359
	C6	-0,00812	0,101804	-0,16911	0,109927	0,160991	0,122312	0,401129
	C11	0,142463	0,224423	0,084005	0,08196	0,058458	0,145655	0,091194
	C14	0,10421	0,115927	0,085447	0,011717	0,018763	0,013037	0,04675
	N 15	-0,28134	-0,24326	-0,31914	0,038078	0,037804	0,042368	0,094193
	C16	0,036763	0,173123	-0,03814	0,13636	0,074907	0,151723	0,18664
B2	C1	0,003129	0,03324	-0,17881	0,030111	0,181943	0,033518	0,53687
	C2	0,005759	0,124064	-0,14472	0,118305	0,150478	0,131692	0,444024
	C3	0,011961	0,116426	-0,16568	0,104465	0,177639	0,116286	0,52417
	C4	0,007023	0,115626	-0,12655	0,108603	0,133577	0,120892	0,394154
	C5	-0,00615	0,106382	-0,0506	0,112529	0,044451	0,125262	0,131164
	C10	0,116385	0,201786	0,040005	0,085401	0,07638	0,225379	0,095065
	C13	0,09072	0,097325	0,072049	0,006605	0,018671	0,007352	0,055094
	N14	-0,23508	-0,16831	-0,30562	0,066768	0,070536	0,074323	0,208135
	C15	0,072754	0,177572	0,026567	0,104818	0,046187	0,116679	0,136287
	O16	-0,17287	-0,08991	-0,19772	0,082968	0,024841	0,092356	0,0733
	C17	0,106552	0,215879	0,031296	0,109327	0,075256	0,121698	0,222062
B3	C1	0,012319	0,112766	-0,16286	0,100447	0,175181	0,143981	0,39148
	C2	0,014594	0,121659	-0,07542	0,107065	0,090011	0,153468	0,201149
	C3	0,019346	0,119608	-0,15483	0,100262	0,174171	0,143716	0,389223
	C4	0,015213	0,112868	-0,06688	0,097655	0,082094	0,139979	0,183457
	C5	-0,00059	0,105924	-0,08063	0,10651	0,080044	0,152672	0,178876
	C10	0,120654	0,202719	0,019689	0,082065	0,100965	0,225628	0,117632
	C13	0,091106	0,098125	0,073745	0,007019	0,017361	0,010061	0,038797
	N14	-0,23124	-0,16602	-0,30381	0,065218	0,072578	0,093484	0,162191
	C15	0,032641	0,124678	-0,04864	0,092037	0,081278	0,131926	0,181633
	Cl16	-0,07405	0,167672	-0,20034	0,241725	0,126289	0,34649	0,28222

The local electrophilicity ω and local nucleophilicity N(ω^-) are reliable parameters related to the most favored electrophile-nucleophile interaction for the formation of a chemical bond between two atoms. The preferred sites for electrophilic attack, in A1 and A2 molecules, are (O19, O20) and (O17, O18)

since they have the highest local nucleophilicity index N(ω^-). C10, C10 and C11 carbons of B1, B2 and B3 molecules are the sensitive sites for nucleophilic attacks since they show the highest values of local electrophilicity ω^+. These results show that the most favored interaction will take place between (O19, O20) and (O17, O18) atoms of A1 and A2 molecules respectively, on the one hand and the C10, C10 and C11 (at the CH_2 alkyl) atoms of B1, B2 and B3 molecules, respectively, on the other hand. The obtained information from the condensed Fukui function is in perfect agreement with the experimentally observed regioselectivity [13].

3.3 Electrostatic potential map (ESP)

The ESP map is very important to determine the information based on the electrophile and nucleophilic reactivity regions of a molecule. It is explained by distinct colors where blue signifies the positive (electron-poor) part, green indicates the neutral part and red denotes the negative (electron-rich) one [34, 35, 36]. **Table 4** shows that the ESP maps of the A1 and A2 alkyl nitroindazole molecules range from -4.316 e^{-2} to +4.316 e^{-2} au for A1 and -4.688 e^{-2} to +4.688 e^{-2} au for A2. We notice that A1 and A2 present a strong negative potential (red color) at the level of the (O19, O20) and (O17, O18) oxygen atoms linked to the nitrogen atom of the aromatic ring and present a weak negative potential (yellowish color) at the level of the nitrogen atom in the heterocyclic system. The ESP map indicates that the electron density is centered on the two oxygen atoms (red region), for A1 and A2, having the highest negative potential making them the preferred site for electrophilic attack.

Table 4 also shows the ESP maps of the aryl acetonitrile molecules (B1, B2 and B3). These ESP maps have the following values: [-5.987 e^{-2} to +5.987 e^{-2} au] for B1, [-5.816 e^{-2} to +5.816 e^{-2} au] for B2, and [-4.931 e^{-2} to +4.931 e^{-2} au] for B3. We notice that B1, B2 and B3 show a strong negative potential (red color) on the nitrogen atom of the (CN) group nitrile, a neutral potential (green color) on the stable aromatic ring system and a positive one (blue region) around the hydrogen atoms of CH_2. This last region presents an electron deficiency (i.e. nucleophilic reactivity) that makes this region a suitable site for intermolecular hydrogen bonding (nucleophilic attack).

Thus the ESP map indicates that the most electron-poor region (blue region) is centered on CH_2 in B1, B2 and B3 reagents. The CH_2 (in aryl acetonitrile) carbon atom has the highest positive potential making it the site favoring the nucleophilic attack.

3.4 Theoretical IR frequencies of the OH and CN functions of the molecules (C1, C2, C3, C4 & C5)

IR spectroscopy has been widely used and as a standard tool for the structural characterization of molecular systems [37, 38]. We have studied the frequencies of organic functions existing in the C1, C2, C3, C4 and C5 synthetized molecules, in order to predict their most stable forms as well as all their possible conformations. This study has been carried out using the B3LYP /6-311G (d, p) theory.

In the 2180-3410 cm^{-1} area in the experimental IR spectra, we determine have the frequencies of the OH and CN functions of the synthetized molecules **(Table 5)**. In the present study, the stretching frequencies of the OH and CN functions for the C1 molecule were observed: a fine peak of high intensity for the OH function and a less intense peak for the CN function with frequencies, respectively, of 3420 cm^{-1} and 2178 cm^{-1} which are close to the experimental frequencies and have differences of 0,005 cm^{-1} and 0,002 cm^{-1}, respectively. The same is observed for all the five synthetized molecules with negligible differences in terms of frequencies. We notice that the experimental frequencies of the infrared spectrum of the five synthesized molecules are similar to the theoretical ones.

Table 4. Electrostatic potential surface of the molecules: A1: 1-Methyl-7-nitro-1H-indazole, A2: 1-Ethyl-7-nitro-1H-indazole, B1: 4-methyl-phenyl-acetonitrile, B2: 4-methoxy-phenyl-acetonitrile and B3: 4-Chloro-phenyl acetonitrile

Molecule	Optimized structure	Electrostatic potential
A1	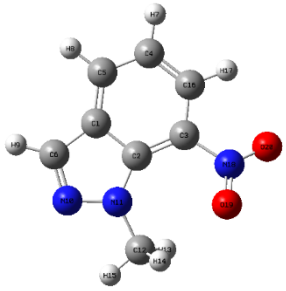	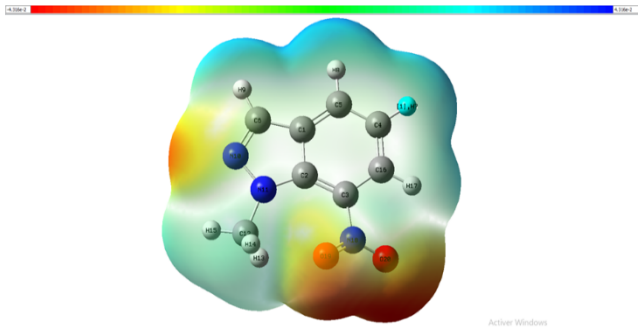
A2	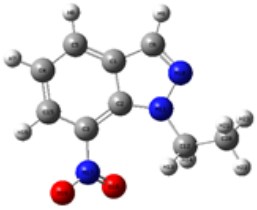	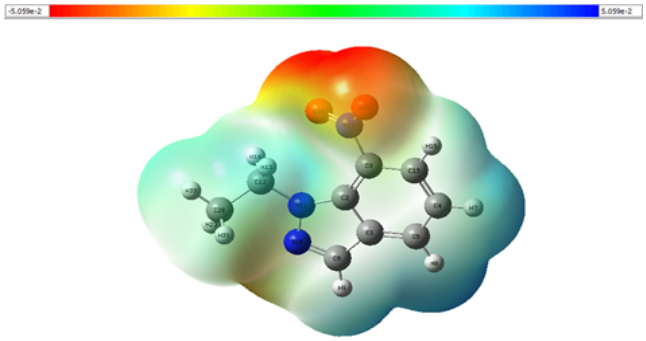
B1	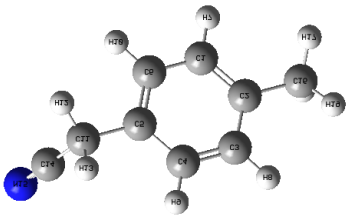	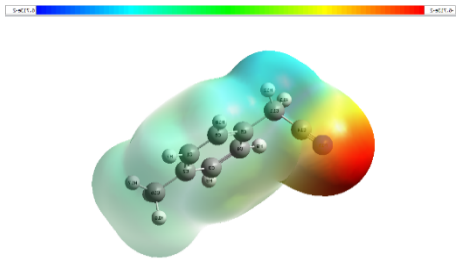
B2	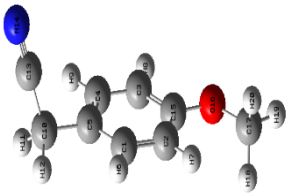	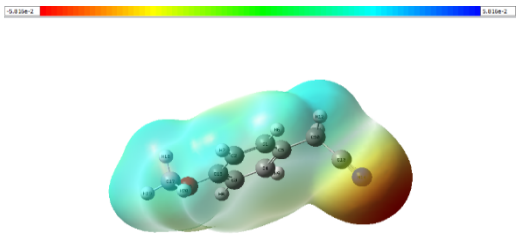
B3	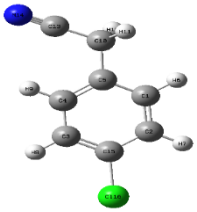	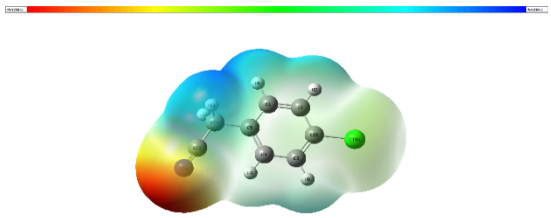

Table 5. Experimental and calculated IR frequencies of C1, C2, C3, C4 and C5 molecules

Molecule	Optimized structure	Function	IR (cm^{-1})	
			Experimental	Calculated
C1	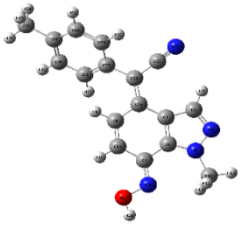	OH	3425	3420
		CN	2180	2178
C2	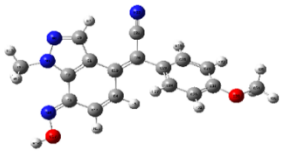	OH	3430	3425
		CN	2204	2200
C3	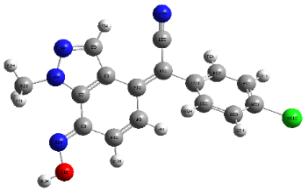	OH	3444	3440
		CN	2190	2185
C4		OH	3450	3448
		CN	2196	2194
C5	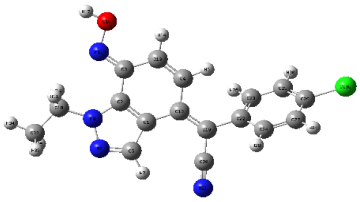	OH	3410	3408
		CN	2182	2180

3.5 Theoretical 1H and 13C NMR chemical shifts of the synthetized molecules

Theoretical calculations of the proton (1H) and carbon (13C) NMR spectra have been performed by the B3LYP /6-311G (d, p) method, whose chemical shifts were calculated by the GIAO (gauge independent atomic orbitals) method, which is the most reliable and recommended by invoking the optimization of the geometry of the molecule [36]. The results show that the NMR range, of chemical shift of the C1, C2, C3, C4 and C5 synthetized molecules, is generally higher than 15 ppm for 13C and lower than 12 ppm for 1H (**Table 6**).

Table 6. Chemical shifts δ (ppm) obtained by the GIAO method of the synthesized molecules (C1, C2, C3, C4 and C5) and experimental (Exp.*) NMR

Molecule	Optimized structure	1H	NMR (δ) Exp.*	NMR (δ) Calculated	13C	NMR (δ) Exp*	NMR (δ) Calculated
C1	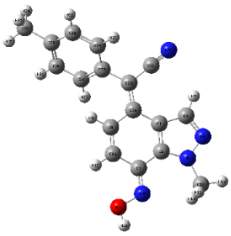	(s, 3H, CH_3)	2.39	2.20	(CH_3)	21.4	21
		(s, 3H, NCH_3)	4.04	4.01	(NCH_3)	40.4	40
		(s, 1H, H-3)	6.40	6.20	(C)	108.3	108
		(d, 1H, *J* = 10.2 Hz)	7.21	7.10	(C)	115.9	114.6
		(m, 4H)	7. 34	7.33	(CH)	118.3	117.9
		(d,1H, *J* = 10.2 Hz)	7.42	7.20	(C)	119.3	119
		(s, 1H, OH)	12.72	12.60	(2CH)	129.3	129.1
					(CH)	129.9	129.4
					(2CH)	130.2	130
					(C)	131.6	131.2
					(C)	134.2	133.2
					(CH)	135.3	135
					(C)	139.1	139.4
					(C)	140.2	140
					(C)	143.3	142.4
C2	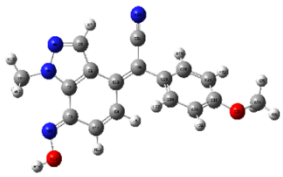	(s, 3H, CH_3O),	3.83	3.90	(NCH_3)	40.7	40
		(s, 3H, NCH_3),	4.04	4.15	(CH_3O)	55.8	55
		(s,1H, H-3),	6.47	6.20	(C)	108.3	107
		(d, 2H, *J* = 8.7Hz),	7.09	6.95	(2CH)	115.5	116.01
		(d, 1H, *J* =9.9 Hz),	7.20	7.20	(C)	115.9	116.
		(d, 1H, *J* = 9.9 Hz),	7.40	7.41	(CH)	118.2	119.5
		(d, 2H, *J* =8.7 Hz),	7.43	7.44	(C)	119.5	120
		(s, 1H, OH);	12.82	12.60	(C)	126.3	125
					(CH)	130.0	129
					(2CH)	131.0	130
					(C)	134.0	133
					(CH)	135.2	136
					(C)	138.8	139.5
					(C)	143.3	140.1
					(C)	160.8	160.1
C3	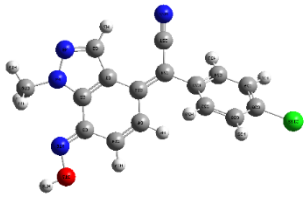	(s, 3H, NCH_3),	4.04	4.01	(NCH_3)	40.5	40.1
		(s, 1H),	6.42	6.49	(C)	108.0	107
		(d, 1H, *J* = 9.9 Hz),	7.22	7.10	(C)	115.8	116
		7.44 (d, 1H, *J* = 9.9 Hz)	7.44	7.20	(CH)	118.2	119
		(d, 2H, *J* = 8.4 Hz)	7.49	7.40	(C)	118.6	118.2
		(d, 2H, *J* = 8.4 Hz),	7.57	7.50	(C)	119.1	119.5
		(s, 1H, OH)	12.94	12.95	(CH)	130.0	131.2
					(2CH)	130.3	131.4
					(2CH)	131.5	132.1
					(C)	131.5	132.0
					(CH)	135.0	134.9
					(C)	138.2	139.1
					(C)	143.0	141.1
C4		(t, 3H, CH_3, *J* = 7.2 Hz),	1.25	1.40	(CH_3)	15.4	15.2
		(s, 3H, CH_3O),	3.83	3.95	(NCH_2)	47.5	49.50
		(q,3H, NCH_2, *J* = 7.2 Hz),	4.46	4.30	(CH_3O)	55.9	57.10
		(s, 1H, H-3),	6.48	6.5	(C)	108.5	108.3
		(d,2H, *J* = 8.7 Hz),	7.07	6.98	(2CH)	115.5	115.2
		(d, 1H, *J* = 9.9 Hz),	7.21	7.20	(C)	116.0	116.8
		(m, 3H),	7.39	7.45	(C)	118.2	117.4
		(s, 1H, OH);	12.82	12.90	(C)	119.5	120.1
					(C)	126.3	125.5
					(CH)	129.9	128.6
					(2CH)	131.0	130.9
					(C)	133.2	134.4
					(CH)	135.4	136.4
					(C)	138.9	139.95
					(C)	143.0	141.5
					(C)	160.8	158.1
C5		(t, 3H, CH_3, *J* = 7.2 Hz),	1.37	1.75	(CH_3)	15.7	15.4
		(q, 3H, NCH_2, J =7.2 Hz)	4.48	4.50	(NCH_2)	48.0	48.1
		(s, 1H)	6.48	6.20	(C)	108.6	104
		(d, 1H, *J* = 9.9 Hz),	7.20	7.10	(C)	116.0	115
		(d,1H, *J* = 9.9 Hz),	7.41	4.30	(CH)	118.3	117.1
		(d, 2H, *J* = 8.4 Hz),	7.46	7.43	(C)	118.7	120.0
		(d, 2H,*J* = 8.4 Hz)	7.58	7.56	(C)	119.3	120.5
		(s, 1H, OH);	12.88	12.95	(CH)	129.9	128.5
					(2CH)	130.5	129.1
					(2CH)	131.3	131.4
					(C)	131.7	131.5
					(CH)	135.2	134.4
					(C)	137.8	138.2
					(C)	143.2	142.5

This result ensures a good precision for the interpretation of the spectroscopic parameters. The experimental and calculated 1H and 13C NMR chemical shifts of the C1, C2, C3, C4 and C5

synthetized molecules, are given in **table 6**. According to these results, the calculated chemical shifts are in accord with the experimental data. As shown in table 6, we plotted the curves of experimental chemical shifts versus those calculated (**Figure 2**).

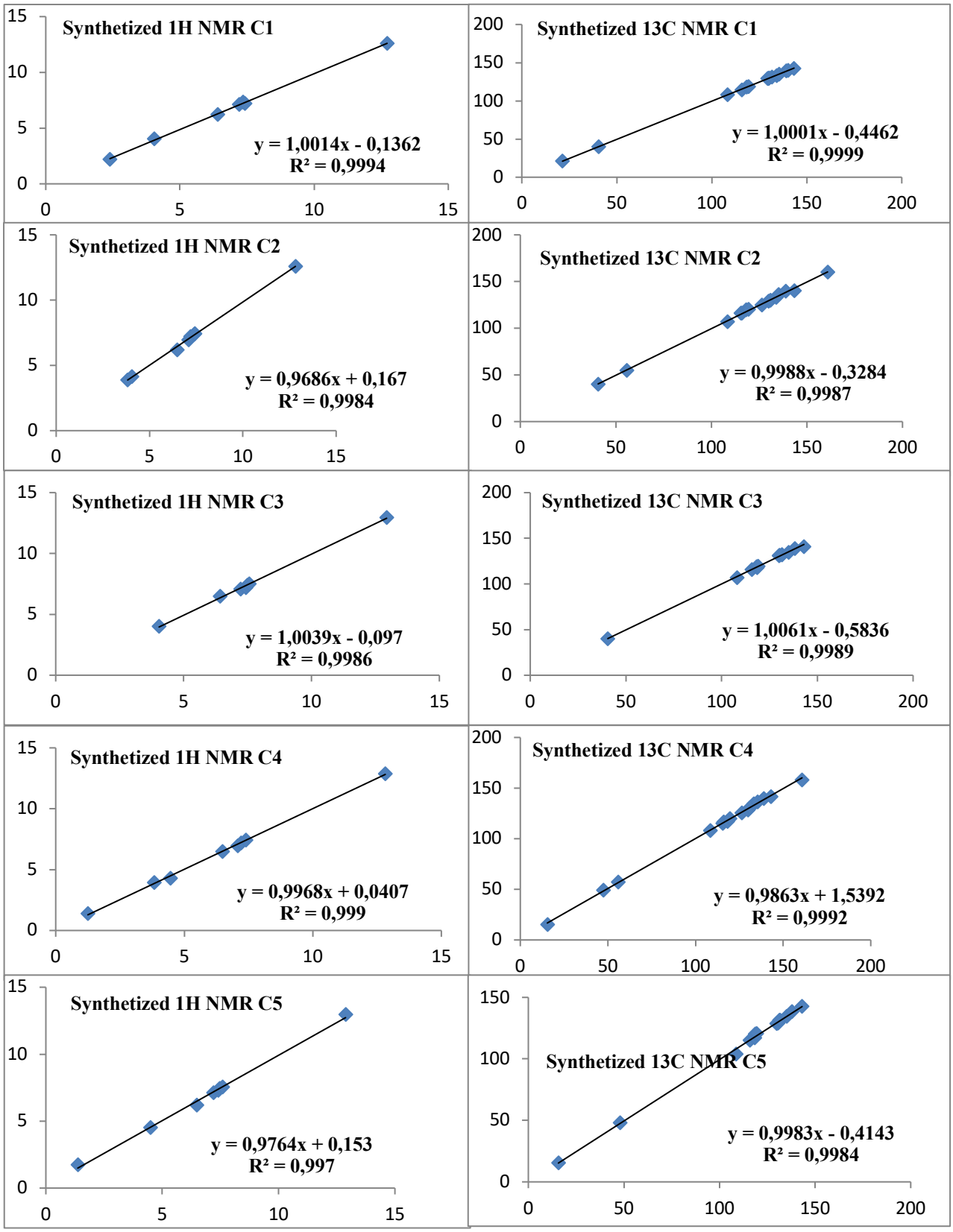

Figure2. Correlation between the experimental and calculated 1H and 13C NMR chemical shifts of the C1, C2, C3, C4 and C5 synthetized molecules

Regarding 1H NMR shifts, the analysis of the linear regression shows a slope equal to 1.001, 0.969, 1.004, 0.997 and 0.976, respectively with the C1, C2, C3, C4 and C5 synthetized molecules. Regarding 13C NMR shifts, the analysis of the linear regression shows a slope equal to 1.000, 0.999, 1.006, 0.986 and 0.9998, respectively with the C1, C2, C3, C4 and C5 synthetized molecules.
The 1H NMR analysis has shown the linearity between calculated and experimental values. The regression coefficient is R^2=0.999, 0.998, 0.999, 0.999 and 0.997 respectively to the C1, C2, C3, C4 and C5 synthetized molecules. The 13C NMR analysis has, also, shown the linearity between calculated and experimental values. The regression coefficient is R^2=0.9999, 0.999, 0.999, 0.999 and 0.998 respectively to the C1, C2, C3, C4 and C5 synthetized molecules. One can observes a concordance between the experimental 1H and 13C NMR results of chemical shifts on the one hand and those theoretically determined on the other hand, using the GIAO method (**Figure 2**).

Conclusion

The regioselectivities of electrophilic-nucleophilic reactions have been studied using the local nucleophilic and electrophilic indices. Our results show that the experimental regioselectivities are correctly reproduced by the Fukui function. Indeed, the local nucleophilicity index predicts that two oxygen atoms in each alkyl nitroindazole reactant are more reactive. A defined carbon from each of the three aryl acetonitrile reactants has the highest electrophilic index. Thus, the present work has been able to highlight the most active sites. These results are consistent with those obtained using the electrostatic potential maps.
The spectroscopic results in terms of 1H and 13C NMR chemical shifts and IR frequencies of the CN and OH functions in the molecules synthetized by the reaction between alkyl nitroindazole and aryl acetonitrile, obtained by calculations are in agreement with the experimental results.
Thus the DFT method is able to guide and optimize the synthesis in organic chemistry thanks to its prediction of the reactivity of molecules both in terms of local and global descriptors and in terms of spectroscopic characteristics such as the chemical displacement and frequencies of organic functions.

References

1. H. Cerecetto, A. Gerpe, M. Gonzalez, V. Aran, C. Ocariz, Pharmacological Properties of Indazole Derivatives: Recent Developments, *European Journal of Medicinal Chemistry*, 5 (2005) 869-878. https://doi.org/10.2174/138955705774329564
2. D. D. Gaikwad, A. D. Chapolikar, C. G. Devkate, K. D. Warad, A.P. Tayade, R. P. Pawar, A. J. Domb, Synthesis of indazole motifs and their medicinal importance, *European Journal of Medicinal Chemistry*, (2015) 707-731. https://doi.org/10.1016/j.ejmech.2014.11.029
3. A. Jennings, M. Tennant, Selection of molecules based on shape and electrostatic similarity: Proof of concept of electroforms, *Journal of Chemical Information and Modeling*, 47 (2007) 1829–1838. https://doi.org/10.1021/ci600549q
4. W. Han, J. C. Pelletier, C. N. Hodge, Tricylic ureas: A new class of HIV-1 protease inhibitors, *Bioorganic Medicinal & Chemistry Letters* 8 (1998) 3615-3620. https://doi.org/10.1016/S0960-894X(98)00659-3
5. S. Vidyacharan, A. Murugan, D. S. Sharada, C(sp2)-H Functionalization of 2H-Indazoles at C3-Position via Palladium(II)-Catalyzed Isocyanide Insertion Strategy Leading to Diverse Heterocycles, *Journal of Organic Chemistry*, 81 (2016) 2837-2848. https://doi.org/10.1021/acs.joc.6b00048

6. H. Saber, A. G Thrift, M. Kapral, Incidence, recurrence, and long-term survival of ischemic stroke subtypes: A population-based study in the Middle East, *International Journal of Stroke*, 0(0) (2017) 835-843. https://doi.org/10.1177/1747493016684843
7. G. Bogonda, H. Y. Kim, K. Oh, Direct Acyl Radical Addition to 2 H-Indazoles Using Ag-Catalyzed Decarboxylative Cross-Coupling of α-Keto Acids, *Organic Letters*, (2018) 2711-2715. https://doi.org/10.1021/acs.orglett.8b00920
8. I. Bouillon, J. Zajíček, N. Pudelová, V. Krchňák, Remarkably efficient synthesis of 2H-indazole 1-oxides and 2H-indazoles via tandem carbon-carbon followed by nitrogen-nitrogen bond formation, *Journal of Organic Chemistry*, 73 (2008) 9027-9032. https://doi.org/10.1021/jo8018895
9. M. E. Tedder, Z. Nie, S Margosiak, S. Chu and V. A. Feher, Structure-based design, synthesis, and antimicrobial activity of purine derived SAH/MTA nucleosidase inhibitors, *Bioorganic & Medicinal Chemistry Letters*, 14 (2004) 3165-3168. https://doi.org/10.1016/j.bmcl.2004.04.006
10. H. Takahashi, M Shinoyama, T. Komine, M. Nagao, M.Suzuki, H. Tsuchida and K. Katsuyama , Novel dihydrothieno[2,3-e]indazole derivatives as IκB kinase inhibitors, *Bioorganic & Medicinal Chemistry Letters*, 21 (2011) 1758-1762. https://doi.org/10.1016/j.bmcl.2011.01.069
11. F. Y. Le, J.C. Lien, L. J. Huang, T. M. Huang, S. T. sai, C. M. Teng, Synthesis of 1-benzyl-3-(5′-hydroxymethyl-2′-furyl)indazole analogues as novel antiplatelet agents, *Journal of Medicinal Chemistry* , 44 (2001) 3746-3749. https://doi.org/10.1021/jm010001h
12. O. Rosati, M. C. Marcotullio, A. Macchiarulo, M. Perfumi, L. Mattioli, F. Rismondob, G. Cravottoc , Synthesis , docking studies and anti-inflammatory activity of 4 , 5 , 6 , 7-tetrahydro-2 H -indazole derivatives, *Bioorganic & Medicinal Chemistry*, 15 (2007) 3463-3473. https://doi.org/10.1016/j.bmc.2007.03.006
13. A. Kouakou, N. Abbassi, H. Chicha, L. El Ammari, M. Saadi, E. M. Rakib, Synthesis of Novel Substituted Indazoles via Nucleophilic Substitution of Hydrogen (S N H), *ChemInform*, 26 (2016), 374-381. https://doi.org/10.1002/chin.201602117
14. F. E. Laghchioua, A. Kouakou, M. Eddahmi, M. Viale, M. Monticone, R. Gangemi, I. Maric, L. El Ammari, M.Saadi3, M. Baltas, Y, Kandri Rodi, El M. Rakib, Antiproliferative and apoptotic activity of new indazole derivatives as potential anticancer agents, *Archiv der Pharmazie. (Weinheim)*, (2020) 1-11. https://doi.org/10.1002/ardp.202000173
15. L. Bouissane, S. El Kazzouli, S. L. once, B. Pfeiffer, E. M. Rakib, M. Khouilib, G. Guillaumet, Synthesis and biological evaluation of N-(7-indazolyl)benzenesulfonamide derivatives as potent cell cycle inhibitors, *Bioorganic & Medicinal Chemistry*, 14 (2006) 1078-1088. https://doi.org/10.1016/j.bmc.2005.09.037
16 S. V. Patil, K. P. Nandre , S. Ghosh , V. J. Rao , B. A. Chopade , S. V. Bhosale , S. V. Bhosale, Synthesis and glycosidase inhibitory activity of novel (2-phenyl-4H-benzopyrimedo[2,1-b]-thiazol-4-yliden)acetonitrile derivatives, *Bioorganic & Medicinal Chemistry,22 (2012) 7011-7014*. https://doi.org/10.1016/j.bmcl.2012.10.025
17 M. R. Rich, L. A. Dulay, J. S. Miranda, S. P. Malasaga, R. G. Kalaw, C. T. Reyes, Antioxidant and Antibacterial Activities of Acetonitrile and Hexane Extracts of Lentinus tigrinus and Pleurotus djamour, Biocatalysis and Agricultural Biotechnology, *Biocatalysis and Agricultural Biotechnology*, 9 (2017) 141-144.
18. A. P. Scott, L. Radom, Harmonic vibrational frequencies: An evaluation of Hartree-Fock,

Møller-Plesset, quadratic configuration interaction, density functional theory, and semiempirical scale factors, *Journal of Physical Chemistry*, 100 (1996) 16502-16513. https://doi.org/10.1021/jp960976r
19. E. J. Ocola, T. Brito, K. McCann, J. Laane, Conformational energetics and low-frequency vibrations of cyclohexene and its oxygen analogs, *Journal of Molecular Structure*, 978 (2010) 74-78. https://doi.org/10.1016/j.molstruc.2009.11.026
20. S. Breda, I. Reva, R. Fausto, Molecular structure and vibrational spectra of 2(5H)-furanone and 2(5H)-thiophenone isolated in low temperature inert matrix, *Journal of Molecular Structure*, 887 (2008) 75-86 https://doi.org/10.1016/j.molstruc.2008.02.034
21. H. E. L. Ouafy, T. E. L. Ouafy, M. Oubenali, M. Mbarki, A. E. L. Haimouti, M. Echajia, Evaluation by NMR spectroscopy and global descriptors of the para substituents of aniline by the DFT method, *Journal of Materials and Environmental Science* , 12 (2021) 104-114.
22. T. Schwabe, S. Grimme, Towards chemical accuracy for the thermodynamics of large molecules: New hybrid density functionals including non-local correlation effects, *Physical Chemistry Chemical Physics*, 8 (2006) 4398-4401. https://doi.org/10.1039/b608478h
23. J. R. Durig, A. Ganguly, A. M. El Defrawy, T. K. Gounev, G. A. Guirgis, Conformational stability of cyclobutanol from temperature dependent infrared spectra of xenon solutions, structural parameters, ab initio calculations and vibrational assignment, *Spectrochimica Acta - Part,* 71 (2008)1379-1389. https://doi.org/10.1016/j.saa.2008.04.010
24. P. Thanikaivelan, V. Subramanian, J. Raghava Rao, B. U. Nair, Application of quantum chemical descriptor in quantitative structure activity and structure property relationship, *Chemical Physics, 323 (2000) 59–70*. 10.1016/S0009-2614(00)00488-7
25. F. De Proft, R. Vivas-Reyes, M. Biesemans, R. Willem, J. M. L. Martin, P. Geerlings, Density Functional Study of the Complexation Reaction of Sn(CH 3)3X (X = F, Cl, Br and I) with Halide Anions, *European Journal of Inorganic Chemistry*, (2003) 3803-3810. https://doi.org/10.1002/ejic.200300044
26. R. G. Pearson, Hard and Soft Acids and Bases, *American Chemical Society*, 85 (1963) 3533-3539. https://doi.org/10.1021/ja00905a001
27. R. G. Pearson, Absolute electronegativity and hardness correlated with molecular orbital theory, *Proceedings of the National Academy of Sciences*, 83 (1986) 8440-8441. https://doi.org/10.1073/pnas.83.22.8440
28. R. G. Parr, R. G. Pearson, Absolute Hardness: Companion Parameter to Absolute Electronegativity, *Journal of the American Chemical Society*, 105 (1983) 7512-7516. https://doi.org/10.1021/ja00364a005
29. L. R. Domingo, M. J. Aurell, P. Pérez, R. Contreras, Quantitative characterization of the global electrophilicity power of common diene/dienophile pairs in Diels-Alder reactions, *Tetrahedron*, 58 (2002) 4417-4423. https://doi.org/10.1016/S0040-4020(02)00410-6
30. L. R. Domingo, E. Chamorro, P. Pérez, Understanding the reactivity of captodative ethylenes in polar cycloaddition reactions. A theoretical study, *Journal of Organic Chemistry*, 73 (2008) 4615-4624. https://doi.org/10.1021/jo800572a
31. L. Feng, H. Yang, and F. Wang, Experimental and theoretical studies for corrosion inhibition of carbon steel by imidazoline derivative in 5% NaCl saturated Ca(OH)2 solution, *Electrochimica Acta*, 58 (2011) 427-436. https://doi.org/10.1016/j.electacta.2011.09.063
32. S. Rameshkumar, I. Danaee, M. RashvandAvei, M. Vijayan, Quantum chemical and

experimental investigations on equipotent effects of (+)R and (-)S enantiomers of racemic amisulpride as eco-friendly corrosion inhibitors for mild steel in acidic solution, *Journal of Molecular Liquids*, 212 (2015)168-186. https://doi.org/10.1016/j.molliq.2015.09.001

33. R. Parthasarathi, J. Padmanabhan, U. Sarkar, B. Maiti, V.Subramanian, P. Kumar Chattaraj, Toxicity Analysis of Benzidine Through Chemical Reactivity and Selectivity Profiles: A DFT Approach, *of Molecular Design* 2 (2003) 798–813
34. M. Arivazhagan , S. Jeyavijayan, Vibrational spectroscopic, first-order hyperpolarizability and HOMO, LUMO studies of 1,2-dichloro-4-nitrobenzene based on Hartree-Fock and DFT calculations, *Spectrochimica Acta Part,* 79 (2011) 376-383. https://doi.org/10.1016/j.saa.2011.03.036
35. M. Arivazhagan, G. Thilagavathi, Vibrational study, first hyperpolarizability and HOMO-LUMO analyses on the structure of 2-hydroxy-6-nitro toluene, *Spectrochimica Acta Part*, 91 (2012) 411-418. https://doi.org/10.1016/j.saa.2012.02.025
36. N. Sundaraganesan, J. Karpagam, S. Sebastian, J. P. Cornard, The spectroscopic (FTIR, FT-IR gas phase and FT-Raman), first order hyperpolarizabilities, NMR analysis of 2,4-dichloroaniline by ab initio HF and density functional methods, *Spectrochimica Acta Part*, 73 (2009) 11-19. https://doi.org/10.1016/j.saa.2009.01.007
37. S. Singh, A. Srivastavaa, P. Tandona, R. Debb, S. Debnathb, N.V.S. Raob , A.P. Ayala, Study of phase transitions in a bent-core liquid crystal probed by infrared spectroscopy, *Vibrational Spectroscopy* , 86 (2016) 24-34. https://doi.org/10.1016/j.vibspec.2016.05.005
38. S. Singh, H. Singh, T. Karthick, P. Agarwal, R. D. Erande, D. H. Dethe, P. Tandon, Combine experimental and theoretical investigation on an alkaloid-Dimethylisoborreverine, *Journal of Molecular Structure*, (2016) 187-201. https://doi.org/10.1016/j.molstruc.2015.09.021

(2022) ; http://www.jmaterenvironsci.com